

Thinking Like a Doctor: Conversational Diagnosis through the Exploration of Diagnostic Knowledge Graphs

Jeongmoon Won* Seungwon Kook* Yohan Jo†

Graduate School of Data Science, Seoul National University

{jmwon06231, cacu5615, yohan.jo}@snu.ac.kr

Abstract

Conversational diagnosis requires multi-turn history-taking, where an agent asks clarifying questions to refine differential diagnoses under incomplete information. Existing approaches often rely on the parametric knowledge of a model or assume that patients provide rich and concrete information, which is unrealistic. To address these limitations, we propose a conversational diagnosis system that explores a diagnostic knowledge graph to reason in two steps: (i) generating diagnostic hypotheses from the dialogue context, and (ii) verifying hypotheses through clarifying questions, which are repeated until a final diagnosis is reached. Since evaluating the system requires a realistic patient simulator that responds to the system’s questions, we adopt a well-established simulator along with patient profiles from MIMIC-IV. We further adapt it to describe symptoms vaguely to reflect real-world patients during early clinical encounters. Experiments show improved diagnostic accuracy and efficiency over strong baselines, and evaluations by physicians support the realism of our simulator and the clinical utility of the generated questions. Our code will be released upon publication.

1 Introduction

The advent of large language models (LLMs) has significantly advanced the medical domain, demonstrating expert-level capabilities on medical benchmarks (Lacerda et al., 2025; Nori et al., 2025; Singhal et al., 2025). However, these benchmarks evaluate LLMs primarily in static, single-turn question-answering (QA) settings, which do not reflect real-world clinical diagnosis. Unlike standardized tasks where complete information is provided upfront, conversational diagnosis is a multi-turn process in which clinicians interact

with patients to narrow down differential diagnoses by eliciting missing information. In this setting, the core challenge is not merely interpreting given facts but proactively and efficiently gathering diagnostically relevant evidence across turns.

Conversational diagnosis systems in such settings can serve as decision-support tools for outpatient initial consultations, where history-taking is often the primary source of diagnostic evidence. A major obstacle, however, is that patients often describe symptoms in vague, incomplete, or underspecified terms (e.g., “my belly feels weird”) (Redelmeier et al., 2001; Dahm et al., 2023; Gaber et al., 2025), which increases the risk of misdiagnosis. Diagnostic accuracy therefore depends on asking the right *clarifying questions* (CQs)—those that effectively target uncertainty and elicit diagnostically relevant cues. As illustrated in Figure 1, direct answers often lead to generic responses (Figure 1a), whereas iterative clarification enables more precise diagnosis (Figure 1b).

Recent work has explored multi-turn conversational diagnosis with CQs through two primary directions, but important limitations remain. Fine-tuned or prompting-based methods (Lai et al., 2025; Feng et al., 2025; Li et al., 2024) often lack explicit grounding in external diagnostic knowledge, making it unclear whether the generated CQs are diagnostically justified. RAG-based approaches leverage external documents relevant to patient utterances to guide CQ generation and diagnosis (Sun et al., 2025; Xu et al., 2024), but are often evaluated in settings where patients provide rich context upfront. This assumption is misaligned with history-taking, where patients reveal information gradually rather than all at once.

In practice, clinicians form a small set of plausible *diagnostic hypotheses* from early cues and iteratively verify or rule them out through targeted CQs (Yuan, 2024; Yazdani et al., 2017; Croskerry, 2009; Norman et al., 2024). This process is typ-

*Equal contribution.

†Corresponding author.

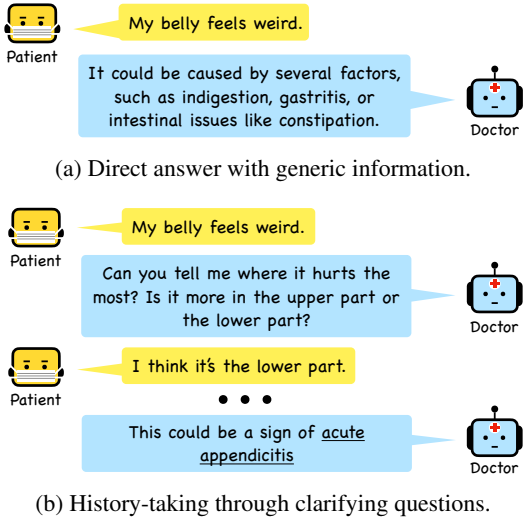


Figure 1: Conceptual comparison between two diagnostic settings.

ically guided by diagnostic knowledge that organizes which cues are informative for distinguishing among competing hypotheses. To support this reasoning in a conversational system, diagnostic knowledge must be represented in a form that allows explicit cross-disease comparison, which we instantiate as a *diagnostic knowledge graph*.

Accordingly, we propose a conversational diagnosis system that operates in two steps: (i) generating plausible hypotheses and extracting a hypothesis-driven subgraph from the diagnostic knowledge graph, and (ii) using the accumulated evidence and dialogue history to generate either a CQ or a final diagnosis. To assess whether the system can actively compensate for underspecified patient utterances through targeted CQs, we build on an existing patient simulator and augment it to model low-specificity symptom reporting.

Empirically, we find that grounding conversational diagnosis in the diagnostic knowledge graph leads to more accurate and efficient diagnosis. Specifically, grounding diagnosis in the graph substantially improves performance over relying on parametric knowledge alone. Moreover, generating CQs based on a small set of plausible hypotheses leads to more targeted and informative CQs. Models trained under this system also achieve stronger diagnostic performance with fewer dialogue turns, indicating more focused and efficient history-taking. Furthermore, qualitative feedback from medical experts confirms that the resulting diagnostic workflows and question sequences are clinically plausible and effective at narrowing

down competing hypotheses. These findings suggest that hypothesis-driven graph grounding provides a practical design principle for building reliable conversational diagnosis systems. Our system can potentially support preliminary diagnosis and patient triage in time-constrained clinical settings, as well as assist clinicians in asking critical questions under heavy workload.

2 Related Work

Prior work has explored conversational diagnosis as a multi-turn process in which a system asks CQs to collect missing evidence before diagnosing. However, we found two recurring limitations. The first limitation concerns assumptions about patient behavior. Some retrieval-augmented approaches implicitly assume that patients provide rich and informative context upfront, thereby overlooking the reality of early-stage history-taking, where patient descriptions are often vague or underspecified (Sun et al., 2025; Xu et al., 2024). Other policy-optimization approaches simplify interaction by restricting patient responses to three choices (e.g., yes/no/unknown) (Jia et al., 2025; Sun et al., 2024). This setting requires an excessive number of granular CQs that must be answerable with yes/no (e.g., asking for a location via separate queries for upper, lower, left, and right). In contrast, our system is designed to operate under vague or underspecified patient utterances.

The second limitation concerns how systems leverage medical knowledge. Some recent fine-tuned or prompting-based models primarily rely on parametric knowledge without explicit external grounding, making their CQs and diagnoses difficult to verify (Lai et al., 2025; Feng et al., 2025; Li et al., 2024). Other work incorporates knowledge graphs, but often uses them only for disease scoring or entity-level retrieval rather than for guiding discriminative questioning (Chen et al., 2025; Wu et al., 2024). Our system addresses this gap by explicitly grounding CQ generation and diagnosis decisions in structured diagnostic knowledge.

3 Methodology

3.1 Problem Definition

Let $\mathcal{D} = [(u_1^P, u_1^D), \dots, (u_T^P, u_T^D)]$ denote a dialogue session, where u_t^P and u_t^D represent the patient utterance and system response at turn t , respectively. The system response u_t^D takes the

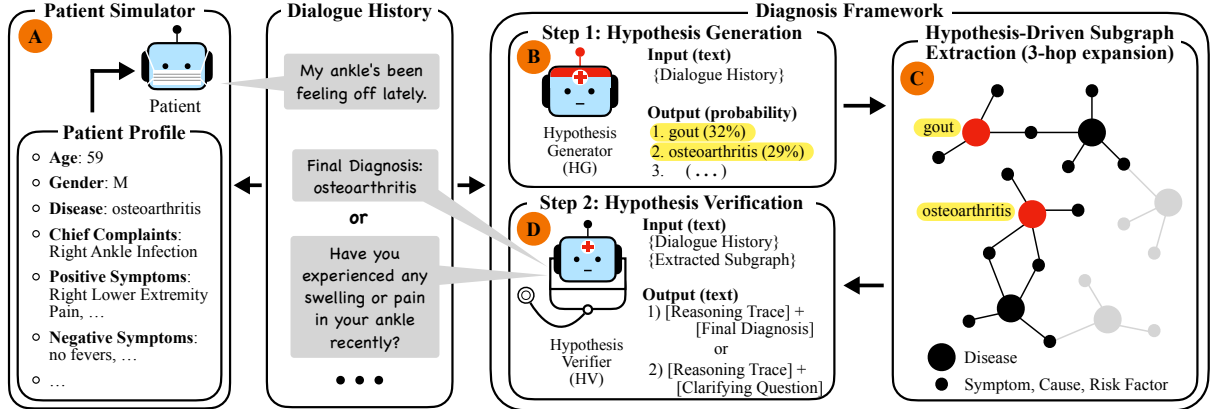


Figure 2: Our system (i) generates diagnostic hypotheses from the dialogue context (§3.3.1), and (ii) verifies hypotheses through clarifying questions, which are repeated until the final diagnosis (§3.3.2).

form of either a CQ or a final diagnosis. We define the dialogue history up to turn t as $H_t = (u_1^P, u_1^D, \dots, u_t^P)$. Given H_t and a diagnostic knowledge graph \mathcal{G} , our objective is to generate an optimal response u_t^D that minimizes diagnostic uncertainty and leads to the correct identification of the ground-truth disease d_{gold} . Figure 2 provides an overview of our system.

3.2 Diagnostic Knowledge Graph

We construct a diagnostic knowledge graph \mathcal{G} that provides structured medical grounding to support diagnostic hypothesis generation and verification through CQs. While existing biomedical knowledge graphs (Bodenreider, 2004; Chandak et al., 2023) offer broad and expert-level medical knowledge, their wide scope often introduces extraneous information that acts as noise during diagnostic reasoning (Zhai et al., 2024; Mavi et al., 2023). Instead, we derive \mathcal{G} from diagnostic schemas—clinical decision trees commonly used by clinicians and described in standard medical textbooks. However, directly using such schemas is ill-suited for conversational diagnosis, because they organize information separately for each disease. As a result, a system cannot easily reason from a single symptom to the set of competing diseases associated with it, nor compare those diseases to determine which CQs are most discriminative.

To address this limitation, we reformulate disease-specific schemas into a unified graph representation that explicitly supports cross-disease comparison. In this graph, multiple diseases share attribute nodes (symptom, cause, and risk_factor), capturing many-to-many rela-

tionships between diseases and clinical cues. This shared structure enables the system to reason over overlapping and contrasting attributes among candidate diseases, directly supporting discriminative CQ generation during history-taking. The resulting \mathcal{G} contains 338 disease nodes connected to attribute nodes via 3,935 edges. Detailed information about our diagnostic schemas and graph is provided in Appendix A.

3.3 Diagnosis Framework

We model conversational diagnosis as an iterative, hypothesis-driven reasoning process in which the system alternates between generating diagnostic hypotheses and verifying them through CQs.

3.3.1 Step 1: Hypothesis Generation (Figure 2, B)

The goal of this step is to generate a small set of plausible diagnostic hypotheses from the current dialogue history. Each hypothesis corresponds to a candidate disease node in \mathcal{G} and serves as an anchor for subsequent evidence-driven questioning. By first identifying plausible diseases, the system can focus its CQs on the most useful information for hypothesis verification.

Given the dialogue history H_t , we predict probability scores over all diseases defined in \mathcal{G} . We formulate this prediction as a multi-label classification task using a *Hypothesis Generator (HG)*. HG takes H_t as input and computes:

$$P(\text{Disease} | H_t) = \sigma(W \cdot \text{LLM}_{\text{HG}}(H_t) + b), \quad (1)$$

where LLM_{HG} denotes the underlying language model, W and b are the learnable weight matrix and bias of the classification head applied to the

final hidden state of the last token, and σ is the sigmoid function. Based on these scores, we select the top- n diseases with the highest probabilities.

Hypothesis-Driven Subgraph Extraction. (Figure 2, C) The selected top- n diseases are treated as anchor hypotheses (represented by red nodes in Figure 2, C). Relying on anchor hypotheses alone is insufficient for making a diagnosis. At this stage, the predicted probabilities have not yet been verified against concrete clinical evidence: the patient may not exhibit the detailed attributes associated with the anchor hypotheses, and the true diagnosis may be a different disease that shares the same attribute nodes. Effective hypothesis verification therefore requires structured access to the attributes that connect competing diseases and differentiate them from plausible alternatives. To this end, we extract a localized subgraph \mathcal{G}_{sub} that provides the necessary diagnostic context.

We perform a 3-hop expansion starting from the anchor disease nodes. Specifically, the expansion includes: (1) 1-hop: to their direct attributes (`symptom`, `cause`, `risk_factor`); (2) 2-hop: to other diseases sharing these attributes, representing competing hypotheses (large black nodes in Figure 2, C); and (3) 3-hop: to the attributes of those competing diseases. By exposing both shared and disease-specific attributes, this structure enables the system to generate CQs that either strengthen confidence in a plausible hypothesis or rule it out by probing discriminative attributes. To control the size of \mathcal{G}_{sub} , we filter the competing diseases by retaining only those whose predicted probabilities exceed a threshold τ .

3.3.2 Step 2: Hypothesis Verification (Figure 2, D)

In the second step, the *Hypothesis Verifier* (*HV*) validates the candidate diseases identified in Step 1 by actively collecting missing evidence. Given the dialogue history H_t and the extracted subgraph \mathcal{G}_{sub} , the system determines whether to ask a CQ or provide a final diagnosis.

We linearize \mathcal{G}_{sub} into explicit textual statements (e.g., “Disease A causes Symptom B”) and incorporate them into the *HV*’s prompt context. This design enables explicit and interpretable reasoning over diagnostic knowledge without the need to train additional graph encoders, thereby improving generality and ease of integration.

The *HV* then generates an explicit reasoning

trace r_t and a response u_t^D :

$$r_t, u_t^D = \text{LLM}_{\text{HV}}(H_t, \text{Text}(\mathcal{G}_{\text{sub}})). \quad (2)$$

If the *HV* judges the accumulated evidence insufficient, it generates a CQ grounded in \mathcal{G}_{sub} to confirm or rule out specific attributes. Conversely, if the evidence sufficiently supports a hypothesis, the *HV* outputs a final diagnosis. This process iterates, with the patient simulator providing the next utterance u_{t+1}^P , until a diagnosis is reached. The prompt template used for *HV* is in Appendix G.

3.4 Patient Simulator (Figure 2, A)

In our diagnosis framework, we introduce a realistic patient simulator to play the role of a patient that responds to the system’s CQs. At each turn, the simulator takes the underlying patient profile and the CQ as input and generates a response u_t^P . Specifically, it provides an answer when the queried information is available in the profile; otherwise it responds by indicating that the information is uncertain or unknown.

3.4.1 Data Source and Preprocessing

Patient profiles are constructed from the MIMIC-IV dataset suite (Johnson et al., 2024b,a, 2023), a large-scale, de-identified electronic health record dataset. We primarily utilize MIMIC-IV-ED (Emergency Department) (Johnson et al., 2024a), which contains visit-level information such as chief complaints and encounter diagnoses. We augment it with MIMIC-IV-Note (Johnson et al., 2023) to aggregate clinical notes required for constructing detailed patient profiles. Emergency department encounters closely resemble time-constrained initial consultations under incomplete information. This makes our system well-suited to support efficient history-taking and indispensable for reducing patient wait times through automated preliminary diagnosis and patient triage.

Each profile includes (i) basic information (age, gender, chief complaint, and disease labels), (ii) history of present illness, including symptoms asked about during the encounter and whether the patient affirmed or denied them, and (iii) background information such as past medical history, family history, and social history. While most cues (e.g., current symptoms) are readily reportable by patients, some details such as precise medical history may be uncertain; this behavior is modeled through persona and specificity traits as described in the following section (see §3.4.2).

Component	Train	Valid	Test
Hypothesis Generator	1,390	172	174
Hypothesis Verifier	1,449	304	275

Table 1: The number of patient profiles used for training and validation of the HG and HV. The test split is used exclusively for model selection among alternative HG variants.

For these patient profiles, we align MIMIC disease labels with disease nodes in \mathcal{G} . We first apply exact string matching; when an exact match is unavailable, we perform LLM-based semantic matching to map clinically equivalent disease names. Each profile contains between one and four diagnosed diseases. Because our system grounds reasoning in \mathcal{G} , we retain only profiles whose disease labels can be mapped to graph nodes. Profiles that fail this mapping often correspond to secondary conditions or clinical findings rather than well-defined disease entities (e.g., gastrointestinal hemorrhage, syncope) and are thus discarded. The retained profiles still cover major disease categories, including respiratory (e.g., upper respiratory tract infection), gastrointestinal (e.g., acute appendicitis), and dermatologic conditions (e.g., cellulitis). Overall, approximately 28% of the original patient profiles are retained after filtering. Since our primary goal is to investigate how graph grounding supports hypothesis-driven questioning and diagnosis, such cases are beyond the current scope. Importantly, our framework can be adopted as-is with an extended \mathcal{G} to encompass additional diseases.

To mitigate class imbalance, we perform stratified sampling based on disease types and co-occurrence counts when creating train, validation, and test splits. We further limit the number of training profiles to 60 per disease. Dataset statistics are reported in Table 1.

3.4.2 Simulator Adoption and Specificity Augmentation

We adopt PatientSim (Kyung et al., 2025), the persona-driven framework for simulating a patient, as the backbone of our simulator. PatientSim modulates four dimensions of patient behavior: language proficiency, personality, recall level, and confusion level. Each simulated patient is instantiated as a combination of attributes across these dimensions. For example, low proficiency yields short, fragmented utterances; distrustful personas

hesitate to share information; low recall leads to uncertain medical history; high confusion produces tangential or inconsistent responses.

In PatientSim, patient responses often contain sufficient diagnostic details. In real clinical encounters, however, patients frequently fail to provide enough detail, and their symptom descriptions are underspecified (Redelmeier et al., 2001; Dahm et al., 2023). To better reflect this behavior, we instruct the simulator to describe symptoms with low specificity along five symptom-description attributes: *location*, *character*, *duration*, *onset*, and *aggravating/relieving factors*.

To ensure that low-specificity behavior combines naturally with existing personas, we introduce additional prompt components informed by interviews with physicians. Specifically, we (i) restrict the *high recall* persona to past medical history while keeping current symptom descriptions less specific, (ii) allow patients with high language proficiency to exhibit a tendency toward self-diagnosis rather than providing detailed symptom descriptions, and (iii) allow *verbose* personas to mask missing symptom details with long but largely irrelevant text. Prompt templates are provided in Appendix E. In §5.3, we empirically verify that this augmented simulator produces patient behaviors that clinicians perceive as more realistic than the original PatientSim.

3.5 Model Training

3.5.1 Synthetic Dialogue Data Generation

To train the HG and the HV, we need dialogues that reflect iterative history-taking. Therefore, we construct a synthetic dialogues conditioned on each patient profile in the training and validation set. We generate these dialogues by using GPT-4o-mini (OpenAI, 2024) via Azure OpenAI Service, in compliance with PhysioNet’s credentialled data use agreement.¹ We employ two separate instances of GPT-4o-mini to simulate the interaction: one plays the role of the clinician to generate reasoning traces and actions (CQs or diagnoses), while the other serves as the patient simulator (§3.4) when generating patient responses.

During generation, the clinician model is conditioned on the dialogue history and an oracle subgraph $\mathcal{G}_{\text{sub_oracle}}$, which is constructed by performing a 3-hop expansion from d_{gold} . We also pro-

¹<https://physionet.org/news/post/gpt-responsible-use>

vide d_{gold} to ensure medical plausibility during dialogue generation. Importantly, the model is instructed to behave as if the diagnosis is initially unknown and to narrow down hypotheses through iterative questioning.

Although grounding reasoning in \mathcal{G} is central to our system, we do not assume that the model should rely exclusively on the graph. In practice, diagnostic reasoning often requires combining external knowledge with the model’s parametric medical knowledge, especially when patient-provided information is incomplete or weakly covered by the graph. To encourage this adaptive behavior during training, we vary how strongly the model is instructed to rely on the oracle subgraph versus its internal medical knowledge, based on how much of the patient profile is covered by the graph. This allows the model to learn when graph grounding is informative and when flexible use of internal knowledge is necessary. Implementation details are provided in Appendix B.

3.5.2 Training Details

Hypothesis Generator (HG). The HG estimates plausible disease candidates from the current dialogue context. We formulate this as a multi-label classification task, since each patient profile contains between one and four diseases, and use the profile disease labels as ground-truth targets. We initialize LLM_{HG} with Qwen-2.5-7B-Instruct (Yang et al., 2025) and attach a linear classification head to the final hidden state of the last token, mapping to 338 disease labels. At inference time, we rank diseases by predicted probabilities and select the top- n candidates.

We also tested alternative hypothesis generation strategies, including (i) a retrieval-based approach that ranks diseases by embedding similarity to patient-mentioned symptoms and (ii) a generative approach that outputs candidate disease names from the dialogue history. We found the classification-head HG to be more effective. Detailed comparisons and experimental settings are provided in Appendix C.

To support HG at different dialogue stages, we train it on both full dialogues and their truncated ones. Specifically, for each full dialogue, we create multiple sub-dialogues by randomly truncating at intermediate turns. The number of variants is set to 20% of the total dialogue length, and truncation points are sampled uniformly at random. This strategy exposes HG to partial histories of varying

lengths, allowing it to learn hypothesis generation under incomplete evidence.

Hypothesis Verifier (HV). The HV generates reasoning trace and response at each turn. LLM_{HV} is initialized with Qwen-2.5-7B-Instruct and trained via supervised fine-tuning (SFT) on the generated synthetic dialogues. Unlike the HG, the HV is trained on full dialogues without truncation.

The input includes the instruction, the dialogue history H_t , and the extracted subgraph \mathcal{G}_{sub} for the current turn. The output is structured with special tokens: <think> [Reasoning Trace] </think> followed by either <question> [CQ] </question> or <diagnosis> [Final Diagnosis] </diagnosis>. This format enforces explicit reasoning before committing to a question or diagnosis. Example outputs are shown in Appendix H.

4 Experiment Settings

4.1 Baselines

To comprehensively evaluate the effectiveness of our proposed system, we compare it against general-purpose foundation models. In addition, we implemented an adapted version of the Chain-of-Diagnosis (CoD) pipeline (Chen et al., 2025) to benchmark our method against an existing retrieval-based diagnostic framework.

General-Purpose Models. We evaluate performance across general-purpose models: GPT-4.1-mini (OpenAI, 2025), Claude-3.5-Sonnet (Anthropic, 2024), Gemini-2.0-Flash (Google DeepMind, 2024), Llama-3.3-70B (Grattafiori et al., 2024), Qwen-2.5-72B-Instruct (Yang et al., 2025) and Qwen-2.5-7B-Instruct (Yang et al., 2025).

Adapted CoD Baseline. We compare our approach with an adapted version of the Chain-of-Diagnosis (CoD) framework (Chen et al., 2025). The CoD is a multi-turn diagnostic pipeline that retrieves candidate diseases via embedding similarity between patient-mentioned symptoms and disease-associated symptoms, and finalizes the diagnosis once a confidence score over the top-3 candidates exceeds a fixed threshold.

CoD is a suitable baseline because it shares the same high-level structure as our system: both methods (i) identify a small set of plausible disease candidates and (ii) use external medical

knowledge to either ask CQs or output a diagnosis. However, they differ in how knowledge is represented and how the stopping decision is made. During CQ generation, CoD provides the model with disease-centric textual evidence (e.g., disease–symptom/treatment lists) while our method provides the model with subgraph expanded from diagnostic hypotheses. Furthermore, CoD generates a confidence score at each turn and forces termination once this score exceeds a predefined threshold. In our system, by contrast, the model reasons over the dialogue history and the subgraph to decide whether to continue asking CQs or to produce a final diagnosis.

To ensure that both CoD and our framework are grounded in the same underlying medical knowledge, we do not use CoD’s original disease database. Instead, for each candidate disease, we construct CoD’s retrieval context from our \mathcal{G} by extracting the disease node and its 1-hop connected attributes (e.g., symptom, cause, and risk_factor) and providing this information in CoD’s required textual format.

4.2 Experimental Setup

Evaluation Metrics. We evaluate diagnostic accuracy using Recall@ k ($k = 1, 2, 3, 4$), defined as the average proportion of ground-truth diagnoses (d_{gold}) included within the top- k predicted diagnoses across all dialogues. We also measure diagnostic efficiency by the average number of dialogue turns. Because effective history-taking prioritizes a small set of highly informative questions rather than exhaustive inquiry, lower turn counts with comparable accuracy indicate a more practical diagnostic process.

Evaluation Set Details. All results are reported on a held-out test set of 275 patient profiles. Each profile contains up to two ground-truth diseases (252 single-disease cases and 23 double-disease cases). As a result, Recall@1 is theoretically upper-bounded at 0.958, whereas the maximum Recall@ k for $k \geq 2$ is 1.000.

Maximum Turn Limit. To avoid infinite loops, we set a maximum of 50 dialogue turns; sessions exceeding this limit are terminated and counted as failures. This threshold is based on an empirical analysis showing that 91% of patient profiles contain fewer than 50 distinct information units. Since these profiles originate from emergency department records and often include more detail

Models	Recall@ k \uparrow				Turns \downarrow
	1	2	3	4	
GPT-4.1-mini	0.142	0.218	0.218	0.218	<u>7.5</u>
+ KG	<u>0.218</u>	<u>0.319</u>	<u>0.329</u>	<u>0.343</u>	15.3
+ KG + HG	0.243	0.357	0.376	0.383	<u>14.1</u>

Table 2: Ablation study on the impact of the diagnostic knowledge graph and the Hypothesis Generator (HG) on diagnostic performance. Best scores are in **bold**, and second-best scores are underlined.

than required for outpatient initial consultations, informing all recorded symptoms is unnecessary and would be prohibitively burdensome to real patients. We therefore treat 50 turns as sufficient and practical for dialogue-based history-taking.

5 Results

5.1 Diagnostic Performance

Impact of the KG and the HG. To analyze the impact of \mathcal{G} and HG, we conduct an ablation study using GPT-4.1-mini across three settings, as shown in Table 2. Baseline (row 1) relying solely on parametric knowledge achieves Recall@1 of 0.142, indicating limited diagnostic capability. The KG-based variant (row 2) operates without the HG by performing a 2-hop expansion starting from non-disease attribute nodes semantically similar to the patient utterance. The improved Recall@1 of 0.218 demonstrates the benefit of KG grounding. Our full framework (row 3) incorporates the HG to estimate disease probabilities and dynamically filter the extracted subgraph. It achieves the best performance across all metrics (Recall@1–4), increasing Recall@1 to 0.243. These results demonstrate both higher diagnostic accuracy and more efficient diagnosis.

Comparison with Baseline Models. Table 3 compares our SFT model with baselines that incorporate the same HG and \mathcal{G} (except for CoD).

Notably, our SFT model outperforms substantially larger frontier models. It consistently surpasses GPT-4.1-mini across all k values (Recall@1–4). While Claude-3.5-Sonnet achieves the highest Recall@1, it is significantly larger and our model still outperforms it for the remaining metrics (Recall@2–4 and Turns).

Our SFT model significantly outperforms its base model, Qwen2.5-7B-Instruct (Base), across all k values (Recall@1–4), while reducing the average dialogue turns from 12.4 to 6.9. This

Models	Recall@ $k \uparrow$				
	1	2	3	4	Turns \downarrow
<i>Large Models</i>					
GPT-4.1-mini	0.243	<u>0.357</u>	<u>0.376</u>	<u>0.383</u>	14.1
Claude-3.5-Sonnet	0.267	0.329	0.345	0.345	9.4
Gemini-2.0-Flash	0.187	0.241	0.250	0.251	37.0
Llama-3.3-70B	0.186	0.283	0.306	0.313	13.9
Qwen-2.5-72B	0.201	0.255	0.260	0.260	35.2
<i>Small Models (7B)</i>					
CoD	0.106	0.149	0.196	0.207	2.0
Qwen-2.5 (Base)	0.173	0.218	0.218	0.222	12.4
SFT (Ours)	<u>0.250</u>	0.361	0.394	0.418	<u>6.9</u>

Table 3: Diagnostic performance of different models on Recall and the number of Turns. Best scores are in **bold**, and second-best scores are underlined.

demonstrates that fine-tuning on our synthetic diagnostic dialogues enables the model to leverage these components more effectively. The adapted CoD baseline with its optimal confidence threshold terminates too quickly and exhibits lower recall, indicating premature diagnosis. The detailed evaluation results across multiple confidence thresholds are provided in Appendix D.

Error Analysis. We conducted a qualitative analysis to understand the misdiagnosed cases. We identified four primary error patterns: (1) the discrepancy between textbook and real-world patient narratives, (2) the difficulty of diagnosing solely through conversation, (3) confusion between acute and chronic conditions, and (4) limitations arising from label granularity in clinical data. Details are provided in Appendix I.

5.2 Analysis of Hypothesis Generator

Validation of HG Architecture. To validate our architectural choice for the HG, we compare it with three alternatives: (1) a zero-shot generative baseline using GPT-4.1-mini (Gen.); (2) an embedding-based retrieval baseline using SapBERT (Liu et al., 2021) (Retriever), which retrieves disease nodes based on the embedding similarity between patient-reported symptoms and disease symptoms; and (3) a fine-tuned generative baseline based on Qwen-2.5-7B-Instruct (Gen., FT) that directly generates disease names. Recall@ k is computed on truncated dialogues from the HG test split (see § 3.5.2).

As shown in Figure 3, GPT-4.1-mini (Gen.) and SapBERT (Retriever) show limited coverage, suggesting that zero-shot generation or embedding

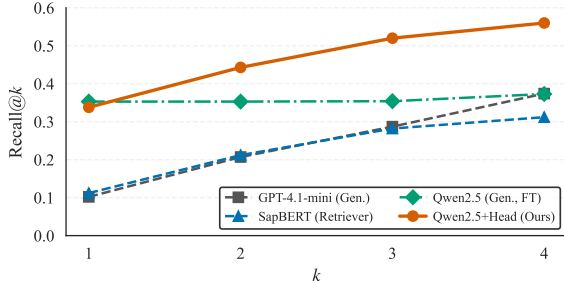


Figure 3: Comparison of disease hypothesis generation performance (Recall@ k) across different methods.

similarity alone is insufficient for handling incomplete multi-turn histories. While the fine-tuned generative baseline, Qwen2.5 (Gen., FT), performs strongly at $k=1$, its improvement plateaus as k increases, indicating a failure to generate reliable candidates for the 2nd to 4th ranks. In contrast, Qwen2.5 + Head (Ours) achieves significantly higher coverage at larger k , reaching a Recall@4 of 0.560. Since subgraph construction incorporates multiple anchor nodes rather than a single selection, high Recall@ k is more critical than Recall@1 to ensure the ground-truth disease is captured within the extracted subgraph. This demonstrates that our classification head provides more reliable ranking, establishing the HG as a robust engine for hypothesis generation.

Impact of the HG Hyperparameters. Table 4 presents the impact of HG hyperparameters on the end-to-end diagnostic performance of our system. Here, n denotes the number of top diseases selected by the HG, and τ denotes the probability threshold used to filter low-confidence disease nodes during subgraph extraction. We calibrated these parameters to ensure that the average number of disease nodes in the extracted subgraphs remained comparable across settings. We report three complementary metrics: (i) *Diagnosis Recall@ k* , which measures whether the ground-truth disease is included in the top- k final diagnoses; (ii) *HG Recall@ k* , the proportion of ground-truth diseases captured within the top- k anchor nodes directly predicted by the HG; and (iii) *Subgraph Recall (Sub Recall)*, which indicates whether the ground-truth disease is contained within the 3-hop subgraph expanded from those anchor nodes. All metrics are computed at the final turn of each dialogue.

The configuration with $n=2$ and $\tau=0.005$

HG Setting	Diagnosis Recall@ $k \uparrow$				Turns ↓	HG Recall@ $k \uparrow$				Sub Recall↑
	1	2	3	4		1	2	3	4	
$n=1, \tau=0.003$	0.204	<u>0.347</u>	0.376	<u>0.411</u>	7.1	0.190	-	-	-	0.538
$n=2, \tau=0.005$	0.250	0.361	<u>0.394</u>	0.418	6.9	0.142	0.256	-	-	0.559
$n=3, \tau=0.01$	0.218	0.305	0.361	0.387	7.2	0.197	0.270	0.317	-	0.482
$n=4, \tau=0.015$	<u>0.229</u>	0.329	0.368	0.418	7.2	0.185	0.277	0.314	0.343	0.423

Table 4: Diagnostic performance of different hyperparameters on 3-hop subgraph expansion setting. Best scores are in **bold**, and second-best scores are underlined.

yields the best performance (*Diagnosis Recall@1* of 0.250 and @4 of 0.418), coinciding with the highest *Sub Recall* of 0.559. Given the controlled subgraph size, this success suggests that concentrating on a few high-confidence anchors ($n=2$) while allowing broad exploration of their neighbors via a lenient threshold ($\tau=0.005$) is more effective for hypothesis verification than distributing attention across a broader set of anchors (i.e., $n=4$, where *Sub Recall* drops to 0.423). This shows that accurately containing the ground-truth disease leads to effective hypothesis verification.

Performance of the Standalone HG. Given that the HG already produces a ranked list of disease candidates, one might question the necessity of the subsequent graph-based reasoning step. To address this, we compare the accuracy of the HG’s hypotheses against the final diagnosis. Table 4 demonstrates that the full pipeline significantly improves upon the HG’s own ranking. In our best configuration ($n=2, \tau=0.005$), the *Diagnosis Recall@1* (0.250) substantially surpasses the *HG Recall@1* (0.142). This gap indicates that the HG serves primarily as a preliminary filter, while reasoning grounded in the extracted subgraph is essential for correcting false positives and refining the diagnostic ranking.

5.3 Evaluation of Patient Simulator

To validate if our specificity-augmented simulator better reflects real-world patients than the original PatientSim, we conducted an expert evaluation.

Experimental Setup. We recruited three board-certified physicians to assess the realism of the patient responses. The evaluation set consisted of 41 distinct dialogues randomly sampled from dialogues generated by our system during inference time. For each scenario, the dialogue history was generated by the baseline PatientSim, and only the last patient response differed between the two sim-

ulators. This ensured both responses were evaluated under the same conversational context. Further details are provided in Appendix J.1.

Results. Across 41 dialogue scenarios, physicians preferred our simulator in 46.3% of cases, compared to 24.4% for the baseline, with 29.3% rated as comparable. Despite the inherent subjectivity of evaluating patient realism, two out of three physicians reached a consensus in 70% of the cases. Among these cases, our simulator was preferred in 75% of the cases. Importantly, this preference emerged even though the preceding dialogue context was generated by the baseline PatientSim. Furthermore, the physicians noted that vagueness in patient responses was a pivotal factor in their preferences for authentic clinical dialogue. This attribution aligns well with our design intent to incorporate low-specificity symptom reporting. Detailed feedback is provided in Appendix J.2.

5.4 Evaluation of CQ Quality

To evaluate the quality of CQs generated by the Hypothesis Verifier (HV), we conducted an interactive human evaluation by medical experts.

Experimental Setup. We recruited four board-certified physicians to participate in interactive diagnostic sessions. Each physician role-played as a patient using 5 unique profiles from the evaluation set, totaling 20 independent sessions. The physicians evaluated CQs on a 5-point Likert scale across three dimensions: *Essentiality* (necessity for diagnosis), *Conversational Flow* (logical progression), and *Clinical Authenticity* (alignment with real-world history-taking), while also providing qualitative feedback to support their evaluations.

Results. Our system scored high in *Clinical Authenticity* (4.25), confirming that CQs closely mirror clinician inquiry patterns. *Essentiality* (3.5) and *Conversational Flow* (3.45) also received pos-

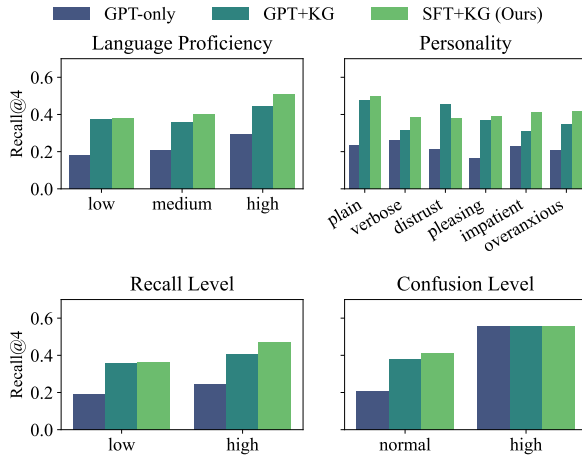


Figure 4: Robustness analysis under diverse patient personas (Recall@4).

itive ratings, indicating moderate efficiency in information gathering. Qualitative feedback highlighted that the overall process of history-taking was clinically natural and appropriate. Furthermore, experts noted that the CQs were strategically targeted toward refining the diagnostic hypotheses identified by HG, even when initial patient descriptions were vague. At the same time, physicians noted that some critical cues (e.g., red-flag symptoms or past medical history) were occasionally underexplored, and that a few candidate diagnoses were less clinically plausible, indicating room for improvement in question prioritization. Detailed evaluation protocols, metrics and qualitative feedback are provided in Appendix K.

5.5 Robustness to Patient Persona Variations

We analyze diagnostic performance across four persona attributes: language proficiency, personality, recall level, and confusion level. We compare three configurations: (i) a baseline relying solely on internal knowledge (GPT-only), (ii) a zero-shot GPT grounded in HG and KG (GPT+KG), and (iii) our fully fine-tuned model grounded in HG and KG (SFT+KG). GPT and SFT denote GPT-4.1-mini and our fine-tuned model (Qwen-2.5-7B-Instruct) respectively.

As shown in Figure 4, KG grounding consistently improves Recall@4 over the GPT-only baseline across all persona variations. Furthermore, the performance gap between our SFT+KG and GPT-only becomes more pronounced as language proficiency decreases. SFT+KG remains competitive across all personality types, including emotionally challenging personas such as *dis-*

trust and *overanxious*. Overall, these results suggest that integrating the KG ensures robust diagnosis even for challenging patient profiles, effectively handling linguistic barriers, emotionally diverse behaviors, and varying memory capabilities. Note that unlike other attributes, the high *confusion* level has a limited sample size, reducing the reliability of the corresponding results.

6 Conclusion

In this work, we presented a conversational diagnosis system designed to support clinical history-taking under incomplete and underspecified patient information. Motivated by how clinicians iteratively refine diagnostic hypotheses through targeted questioning, our system models conversational diagnosis as a two-step process of hypothesis generation and hypothesis verification, grounded in a diagnostic knowledge graph.

Experimental results show that graph grounding substantially improves both diagnostic accuracy and efficiency compared to baselines that rely on parametric knowledge or similarity-based retrieval. In addition, our hypothesis-driven subgraph construction and graph-grounded training strategy improve robustness under diverse patient behaviors. Overall, these findings highlight the potential of combining explicit diagnostic knowledge with interactive language models for reliable and interpretable conversational diagnosis.

7 Limitations

Our work has limitations inherent to its experimental scope. First, we used a patient simulator rather than real-world clinical encounters. This was mainly for ethical considerations regarding testing experimental AI with vulnerable patients, and we instead strengthened our evaluation with patient role-plays performed by physicians. Second, the diagnostic scope is bounded by the current coverage of the diagnostic knowledge graph, which excludes some conditions (including rare diseases). However, this limitation is not fundamental, as the framework can be adopted as-is simply by expanding the graph to incorporate additional diseases and diagnostic cues.

References

Anthropic. 2024. Claude 3.5 sonnet. Anthropic Model Release.

Olivier Bodenreider. 2004. **The unified medical language system (umls): Integrating biomedical terminology.** *Nucleic Acids Research*, 32(Database issue):D267–D270.

Payal Chandak, Kexin Huang, and Marinka Zitnik. 2023. **Building a knowledge graph to enable precision medicine.** *Scientific Data*, 10(1):67.

Junying Chen, Chi Gui, Anningzhe Gao, Ke Ji, Xidong Wang, Xiang Wan, and Benyou Wang. 2025. **CoD, towards an interpretable medical agent using chain of diagnosis.** In *Findings of the Association for Computational Linguistics: ACL 2025*, pages 14345–14368, Vienna, Austria. Association for Computational Linguistics.

Pat Croskerry. 2009. **A universal model of diagnostic reasoning.** *Academic medicine*, 84(8):1022–1028.

Maria R Dahm, William Cattanach, Maureen Williams, Jocelyne M Basseal, Kelly Gleason, and Carmel Crock. 2023. **Communication of diagnostic uncertainty in primary care and its impact on patient experience: an integrative systematic review.** *Journal of general internal medicine*, 38(3):738–754.

Yichun Feng, Jiawei Wang, Lu Zhou, Zhen Lei, and Yixue Li. 2025. **Doctoragent-rl: A multi-agent collaborative reinforcement learning system for multi-turn clinical dialogue.**

Farieda Gaber, Maqsood Shaik, Fabio Allega, Agnes Julia Bilecz, Felix Busch, Kelsey Goon, Vojdran Franke, and Altuna Akalin. 2025. **Evaluating large language model workflows in clinical decision support for triage and referral and diagnosis.** *npj Digital Medicine*, 8(1):263.

Google DeepMind. 2024. **Introducing gemini 2.0: our new ai model for the agentic era.** Google Official Blog.

Aaron Grattafiori, Abhimanyu Dubey, Abhinav Jauhri, Abhinav Pandey, Abhishek Kadian, Ahmad Al-Dahle, Aiesha Letman, Akhil Mathur, Alan Schelten, Alex Vaughan, Amy Yang, Angela Fan, Anirudh Goyal, Anthony Hartshorn, Aobo Yang, Archi Mitra, Archie Sravankumar, Artem Korenev, Arthur Hinsvark, Arun Rao, Aston Zhang, Aurelien Rodriguez, Austen Gregerson, Ava Spataru, Baptiste Roziere, Bethany Biron, Binh Tang, Bobbie Chern, Charlotte Caucheteux, Chaya Nayak, Chloe Bi, Chris Marra, Chris McConnell, Christian Keller, Christophe Touret, Chunyang Wu, Corinne Wong, Cristian Canton Ferrer, Cyrus Nikolaidis, Damien Allonsius, Daniel Song, Danielle Pintz, Danny Livshits, Danny Wyatt, David Esiobu, Dhruv Choudhary, Dhruv Mahajan, Diego Garcia-Olano, Diego Perino, Dieuwke Hupkes, Egor Lakomkin, Ehab AlBadawy, Elina Lobanova, Emily Dinan, Eric Michael Smith, Filip Radenovic, Francisco Guzmán, Frank Zhang, Gabriel Synnaeve, Gabrielle Lee, Georgia Lewis Anderson, Govind Thattai, Graeme Nail, Gregoire Mialon, Guan Pang, Guillem Cucurell, Hailey Nguyen, Hannah Korevaar, Hu Xu, Hugo Touvron, Iliyan Zarov, Imanol Arrieta Ibarra, Isabel Kloumann, Ishan Misra, Ivan Evtimov, Jack Zhang, Jade Copet, Jaewon Lee, Jan Geffert, Jana Vranes, Jason Park, Jay Mahadeokar, Jeet Shah, Jelmer van der Linde, Jennifer Billock, Jenny Hong, Jenya Lee, Jeremy Fu, Jianfeng Chi, Jianyu Huang, Jiawen Liu, Jie Wang, Jiecao Yu, Joanna Bitton, Joe Spisak, Jongsoo Park, Joseph Rocca, Joshua Johnstun, Joshua Saxe, Junteng Jia, Kalyan Vasudevan Alwala, Karthik Prasad, Kartikeya Upasani, Kate Plawiak, Ke Li, Kenneth Heafield, Kevin Stone, Khalid El-Arini, Krithika Iyer, Kshitiz Malik, Kuenley Chiu, Kunal Bhalla, Kushal Lakhota, Lauren Rantala-Yeary, Laurens van der Maaten, Lawrence Chen, Liang Tan, Liz Jenkins, Louis Martin, Lovish Madaan, Lubo Malo, Lukas Blecher, Lukas Landzaat, Luke de Oliveira, Madeline Muzzi, Mahesh Pasupuleti, Mannat Singh, Manohar Paluri, Marcin Kardas, Maria Tsimpoukelli, Mathew Oldham, Mathieu Rita, Maya Pavlova, Melanie Kambadur, Mike Lewis, Min Si, Mitesh Kumar Singh, Mona Hassan, Naman Goyal, Narjes Torabi, Nikolay Bashlykov, Nikolay Bogoychev, Niladri Chatterji, Ning Zhang, Olivier Duchenne, Onur Çelebi, Patrick Alrassy, Pengchuan Zhang, Pengwei Li, Petar Vasic, Peter Weng, Prajjwal Bhargava, Pratik Dubal, Praveen Krishnan, Punit Singh Koura, Puxin Xu, Qing He, Qingxiao Dong, Ragavan Srinivasan, Raj Ganapathy, Ramon Calderer, Ricardo Silveira Cabral, Robert Stojnic, Roberta Raileanu, Rohan Maheswari, Rohit Girdhar, Rohit Patel, Romain Sauvestre, Ronnie Polidoro, Roshan Sumbaly, Ross Taylor, Ruan Silva, Rui Hou, Rui Wang, Saghar Hosseini, Sahana Chennabasappa, Sanjay Singh, Sean Bell, Seohyun Sonia Kim, Sergey Edunov, Shaoliang Nie, Sharan Narang, Sharath Rapparthi, Sheng Shen, Shengye Wan, Shruti Bhosale, Shun Zhang, Simon Vandenhende, Soumya Batra, Spencer Whitman, Sten Sootla, Stephane Collot, Suchin Gururangan, Sydney Borodinsky, Tamar Herman, Tara Fowler, Tarek Sheasha, Thomas Georgiou, Thomas Scialom, Tobias Speckbacher, Todor Mihaylov, Tong Xiao, Ujjwal Karn, Vedanuj Goswami, Vibhor Gupta, Vignesh Ramanathan, Viktor Kerkez, Vincent Gonguet, Virginie Do, Vish Vogeti, Vitor Albiero, Vladan Petrovic, Weiwei Chu, Wenhan Xiong, Wenyin Fu, Whitney Meers, Xavier Martinet, Xiaodong Wang, Xiaofang Wang, Xiaoqing Ellen Tan, Xide Xia, Xinfeng Xie, Xuchao Jia, Xuewei Wang, Yaelle Goldschlag, Yashesh Gaur, Yasmine Babaei, Yi Wen, Yiwu Song, Yuchen Zhang, Yue Li, Yuning Mao, Zacharie Delpierre Coudert, Zheng Yan, Zhengxing Chen, Zoe Papakipos, Aaditya Singh, Aayushi Srivastava, Abha Jain, Adam Kelsey, Adam Shajnfeld, Adithya Gangidi, Adolfo Victoria, Ahuva Goldstand, Ajay Menon, Ajay Sharma, Alex Boesenberg, Alexei Baevski, Allie Feinstein, Amanda Kallet, Amit Sangani, Amos Teo, Anam Yunus, Andrei Lupu, Andres Alvarado, Andrew Caples, Andrew Gu, Andrew Ho, Andrew Poulton, Andrew Ryan, Ankit Ramchandani, Annie Dong, Annie

Franco, Anuj Goyal, Aparajita Saraf, Arkabandhu Chowdhury, Ashley Gabriel, Ashwin Bharambe, Assaf Eisenman, Azadeh Yazdan, Beau James, Ben Maurer, Benjamin Leonhardi, Bernie Huang, Beth Loyd, Beto De Paola, Bhargavi Paranjape, Bing Liu, Bo Wu, Boyu Ni, Braden Hancock, Bram Wasti, Brandon Spence, Brani Stojkovic, Brian Gamido, Britt Montalvo, Carl Parker, Carly Burton, Catalina Mejia, Ce Liu, Changhan Wang, Changkyu Kim, Chao Zhou, Chester Hu, Ching-Hsiang Chu, Chris Cai, Chris Tindal, Christoph Feichtenhofer, Cynthia Gao, Damon Civin, Dana Beaty, Daniel Kreymer, Daniel Li, David Adkins, David Xu, Davide Testuggine, Delia David, Devi Parikh, Diana Liskovich, Didem Foss, Dingkang Wang, Duc Le, Dustin Holland, Edward Dowling, Eissa Jamil, Elaine Montgomery, Eleonora Presani, Emily Hahn, Emily Wood, Eric-Tuan Le, Erik Brinkman, Esteban Arcuate, Evan Dunbar, Evan Smothers, Fei Sun, Felix Kreuk, Feng Tian, Filippos Kokkinos, Firat Ozgenel, Francesco Caggioni, Frank Kanayet, Frank Seide, Gabriela Medina Florez, Gabriella Schwarz, Gada Badeer, Georgia Swee, Gil Halpern, Grant Herman, Grigory Sizov, Guangyi, Zhang, Guna Lakshminarayanan, Hakan Inan, Hamid Shojanazeri, Han Zou, Hannah Wang, Hanwen Zha, Haroun Habeeb, Harrison Rudolph, Helen Suk, Henry Aspegren, Hunter Goldman, Hongyuan Zhan, Ibrahim Damlaj, Igor Molybog, Igor Tufanov, Ilias Leoniadis, Irina-Elena Veliche, Itai Gat, Jake Weissman, James Geboski, James Kohli, Janice Lam, Japhet Asher, Jean-Baptiste Gaya, Jeff Marcus, Jeff Tang, Jennifer Chan, Jenny Zhen, Jeremy Reizenstein, Jeremy Teboul, Jessica Zhong, Jian Jin, Jingyi Yang, Joe Cummings, Jon Carvill, Jon Shepard, Jonathan McPhie, Jonathan Torres, Josh Ginsburg, Junjie Wang, Kai Wu, Kam Hou U, Karan Saxena, Kartikay Khandelwal, Katayoun Zand, Kathy Matosich, Kaushik Veeraraghavan, Kelly Michelena, Keqian Li, Kiran Jagadeesh, Kun Huang, Kunal Chawla, Kyle Huang, Lailin Chen, Lakshya Garg, Laverne A, Leandro Silva, Lee Bell, Lei Zhang, Liangpeng Guo, Licheng Yu, Liron Moshkovich, Luca Wehrstedt, Madian Khabsa, Manav Avalani, Manish Bhatt, Martynas Mankus, Matan Hasson, Matthew Lennie, Matthias Reso, Maxim Groshev, Maxim Naumov, Maya Lathi, Meghan Keneally, Miao Liu, Michael L. Seltzer, Michal Valko, Michelle Restrepo, Mihir Patel, Mik Vyatskov, Mikayel Samvelyan, Mike Clark, Mike Macey, Mike Wang, Miquel Jubert Hermoso, Mo Metanat, Mohammad Rastegari, Munish Bansal, Nandhini Santhanam, Natascha Parks, Natasha White, Navyata Bawa, Nayan Singhal, Nick Egebo, Nicolas Usunier, Nikhil Mehta, Nikolay Pavlovich Laptev, Ning Dong, Norman Cheng, Oleg Chernoguz, Olivia Hart, Omkar Salpekar, Ozlem Kalinli, Parkin Kent, Parth Parekh, Paul Saab, Pavan Balaji, Pedro Rittner, Philip Bontrager, Pierre Roux, Piotr Dollar, Polina Zvyagina, Prashant Ratanchandani, Pritish Yuvraj, Qian Liang, Rachad Alao, Rachel Rodriguez, Rafi Ayub, Raghatham Murthy, Raghu Nayani, Rahul Mitra, Rangaprabhu Parthasarathy, Raymond Li,

Rebekkah Hogan, Robin Battey, Rocky Wang, Russ Howes, Ruty Rinott, Sachin Mehta, Sachin Siby, Sai Jayesh Bondu, Samyak Datta, Sara Chugh, Sara Hunt, Sargun Dhillon, Sasha Sidorov, Satadru Pan, Saurabh Mahajan, Saurabh Verma, Seiji Yamamoto, Sharadh Ramaswamy, Shaun Lindsay, Shaun Lindsay, Sheng Feng, Shenghao Lin, Shengxin Cindy Zha, Shishir Patil, Shiva Shankar, Shuqiang Zhang, Shuqiang Zhang, Sinong Wang, Sneha Agarwal, Soji Sajuyigbe, Soumith Chintala, Stephanie Max, Stephen Chen, Steve Kehoe, Steve Satterfield, Sudarshan Govindaprasad, Sumit Gupta, Summer Deng, Sungmin Cho, Sunny Virk, Suraj Subramanian, Sy Choudhury, Sydney Goldman, Tal Remez, Tamar Glaser, Tamara Best, Thilo Koehler, Thomas Robinson, Tianhe Li, Tianjun Zhang, Tim Matthews, Timothy Chou, Tzook Shaked, Varun Vontimitta, Victoria Ajayi, Victoria Montanez, Viji Mohan, Vinay Satish Kumar, Vishal Mangla, Vlad Ionescu, Vlad Poenaru, Vlad Tiberiu Mihailescu, Vladimir Ivanov, Wei Li, Wenchen Wang, Wenwen Jiang, Wes Bouaziz, Will Constable, Xiaocheng Tang, Xiaojian Wu, Xiaolan Wang, Xilun Wu, Xinbo Gao, Yaniv Kleinman, Yanjun Chen, Ye Hu, Ye Jia, Ye Qi, Yenda Li, Yilin Zhang, Ying Zhang, Yossi Adi, Youngjin Nam, Yu, Wang, Yu Zhao, Yuchen Hao, Yundi Qian, Yunlu Li, Yuzi He, Zach Rait, Zachary DeVito, Zef Rosnbrick, Zhaoduo Wen, Zhenyu Yang, Zhiwei Zhao, and Zhiyu Ma. 2024. [The llama 3 herd of models](#).

Zhihao Jia, Mingyi Jia, Junwen Duan, and Jianxin Wang. 2025. [DDO: Dual-decision optimization for LLM-based medical consultation via multi-agent collaboration](#). In *Proceedings of the 2025 Conference on Empirical Methods in Natural Language Processing*, pages 26369–26386, Suzhou, China. Association for Computational Linguistics.

Alistair Johnson, Lucas Bulgarelli, Tom Pollard, Leo Anthony Celi, Roger Mark, and Steven Horng. 2024a. [Mimic-iv-ed \(version 2.2\)](#). PhysioNet. Version 2.2.

Alistair Johnson, Lucas Bulgarelli, Tom Pollard, Brian Gow, Benjamin Moody, Steven Horng, Leo Anthony Celi, and Roger Mark. 2024b. [Mimic-iv \(version 3.1\)](#). PhysioNet. Version 3.1.

Alistair Johnson, Tom Pollard, Steven Horng, Leo Anthony Celi, and Roger Mark. 2023. [Mimic-iv-note: Deidentified free-text clinical notes \(version 2.2\)](#). PhysioNet. Version 2.2.

Daeun Kyung, Hyunseung Chung, Seongsu Bae, Jiho Kim, Jae Ho Sohn, Taerim Kim, Soo Kyung Kim, and Edward Choi. 2025. [Patientsim: A person-driven simulator for realistic doctor-patient interactions](#). In *The Thirty-ninth Annual Conference on Neural Information Processing Systems Datasets and Benchmarks Track*.

Anisio Lacerda, Gisele Pappa, Adriano César Machado Pereira, Wagner Meira Jr, and Alexandre Guimarães de Almeida Barros. 2025. [Evaluation](#)

of medical large language models: Taxonomy, review, and directions. In *Proceedings of the Thirty-Fourth International Joint Conference on Artificial Intelligence, IJCAI-25*, pages 10528–10536. International Joint Conferences on Artificial Intelligence Organization. Survey Track.

Yunghwei Lai, Kaiming Liu, Ziyue Wang, Weizhi Ma, and Yang Liu. 2025. Doctor-r1: Mastering clinical inquiry with experiential agentic reinforcement learning.

Shuyue Stella Li, Vidhisha Balachandran, Shangbin Feng, Jonathan S. Ilgen, Emma Pierson, Pang Wei Koh, and Yulia Tsvetkov. 2024. Mediq: Question-asking llms and a benchmark for reliable interactive clinical reasoning. In *Advances in Neural Information Processing Systems*, volume 37, pages 28858–28888. Curran Associates, Inc.

Fangyu Liu, Ehsan Shareghi, Zaiqiao Meng, Marco Basaldella, and Nigel Collier. 2021. Self-alignment pretraining for biomedical entity representations. In *Proceedings of the 2021 Conference of the North American Chapter of the Association for Computational Linguistics: Human Language Technologies*, pages 4228–4238, Online. Association for Computational Linguistics.

Vaibhav Mavi, Abulhair Saparov, and Chen Zhao. 2023. Retrieval-augmented chain-of-thought in semi-structured domains. In *Proceedings of the Natural Legal Language Processing Workshop (NLLP) 2023*, pages 178–191. Association for Computational Linguistics.

Harsha Nori, Mayank Daswani, Christopher Kelly, Scott Lundberg, Marco Tulio Ribeiro, Marc Wilson, Xiaoxuan Liu, Viknesh Sounderajah, Jonathan Carlson, Matthew P Lungren, Bay Gross, Peter Hames, Mustafa Suleyman, Dominic King, and Eric Horvitz. 2025. Sequential diagnosis with language models.

Geoff Norman, Thierry Pelaccia, Peter Wyer, and Jonathan Sherbino. 2024. Dual process models of clinical reasoning: the central role of knowledge in diagnostic expertise. *Journal of Evaluation in Clinical Practice*, 30(5):788–796.

OpenAI. 2024. Gpt-4o mini. OpenAI Model Release.

OpenAI. 2025. Gpt-4.1-mini. OpenAI Model Release.

Donald A Redelmeier, Michael J Schull, Janet E Hux, Jack V Tu, and Lorraine E Ferris. 2001. Problems for clinical judgement: 1. eliciting an insightful history of present illness. *Cmaj*, 164(5):647–651.

Karan Singhal, Tao Tu, Juraj Gottweis, Rory Sayres, Ellery Wulczyn, Mohamed Amin, Le Hou, Kevin Clark, Stephen R Pfahl, Heather Cole-Lewis, et al. 2025. Toward expert-level medical question answering with large language models. *Nature Medicine*, 31(3):943–950.

Penglei Sun, Yixiang Chen, Xiang Li, and Xiaowen Chu. 2025. The multi-round diagnostic rag framework for emulating clinical reasoning.

Zhoujian Sun, Cheng Luo, Ziyi Liu, and Zhengxing Huang. 2024. Conversational disease diagnosis via external planner-controlled large language models.

Jiageng Wu, Xian Wu, Yefeng Zheng, and Jie Yang. 2024. Medkp: Medical dialogue with knowledge enhancement and clinical pathway encoding. *arXiv preprint arXiv:2403.06611*. ArXiv:2403.06611 [cs.CL].

Kaishuai Xu, Wenjun Hou, Yi Cheng, Jian Wang, and Wenjie Li. 2024. Medical dialogue generation via intuitive-then-analytical differential diagnosis. *arXiv preprint arXiv:2401.06541*.

An Yang, Baosong Yang, Beichen Zhang, Binyuan Hui, Bo Zheng, Bowen Yu, Chengyuan Li, Dayiheng Liu, Fei Huang, Haoran Wei, Huan Lin, Jian Yang, Jianhong Tu, Jianwei Zhang, Jianxin Yang, Jiaxi Yang, Jingren Zhou, Junyang Lin, Kai Dang, Keming Lu, Keqin Bao, Kexin Yang, Le Yu, Mei Li, Mingfeng Xue, Pei Zhang, Qin Zhu, Rui Men, Runji Lin, Tianhao Li, Tianyi Tang, Tingyu Xia, Xingzhang Ren, Xuancheng Ren, Yang Fan, Yang Su, Yichang Zhang, Yu Wan, Yuqiong Liu, Zeyu Cui, Zhenru Zhang, and Zihan Qiu. 2025. Qwen2.5 technical report.

Shahram Yazdani, Mohammad Hosseinzadeh, and Fakhrolsadat Hosseini. 2017. Models of clinical reasoning with a focus on general practice: a critical review. *Journal of advances in medical education & professionalism*, 5(4):177.

Han Yuan. 2024. Clinical decision making: Evolving from the hypothetico-deductive model to knowledge-enhanced machine learning. *Medicine Advances*, 2(4):375–379.

Weihe Zhai, Arkaitz Zubiaga, Bingquan Liu, Chengjie Sun, and Yalong Zhao. 2024. Towards faithful knowledge graph explanation through deep alignment in commonsense question answering. In *Proceedings of the 2024 Conference on Empirical Methods in Natural Language Processing (EMNLP)*, pages 18920–18930. Association for Computational Linguistics.

A Details of Diagnostic Schemas and Diagnostic Knowledge Graph

Our diagnostic knowledge graph is constructed from diagnostic schemas described in a standard Korean CPX preparation textbook widely used as reference material for the Clinical Performance Examination (CPX) of the Korean Medical Licensing Examination. Specifically, we referenced *10 Minutes CPX*². The textbook covers 48 schemas across major clinical domains, including cardiopulmonary complaints (e.g., cough, chest pain), gastrointestinal complaints (e.g., abdominal pain, hematemesis, diarrhea), neuropsychiatric complaints (e.g., headache, dizziness), musculoskeletal/dermatologic/endocrine complaints (e.g., back pain, rash), genitourinary/obstetric complaints (e.g., dysuria, hematuria), and general systemic symptoms (e.g., weight loss, fever). We exclude the counseling-focused section (e.g., smoking cessation, substance abuse) because it is not aligned with our target setting of outpatient initial consultations. While the textbook also includes additional materials such as recommended examinations, treatment strategies, and example patient cases, our work selectively focuses on the diagnostic schemas for history-taking. This design choice reflects our goal of studying hypothesis-driven questioning during initial diagnostic conversations, rather than downstream testing or treatment decisions.

Each schema provides (i) a differential diagnosis list for the corresponding symptom group and (ii) discriminative history-taking cues (e.g., key symptom attributes, associated findings, risk factors, and related characteristics). As the original schemas are written in Korean, we translated them into English and then reformatted them into a unified graph representation. Based on the translated schemas, we extracted disease nodes and their associated clinical attributes to construct the diagnostic knowledge graph used in our system.

The resulting graph contains four node types: `disease`, `symptom`, `cause`, and `risk_factor`. We define three relation types between these nodes. The `caused_by` relation connects a `symptom` node to a `disease`, indicating that the symptom is a clinical manifestation associated with the disease. The

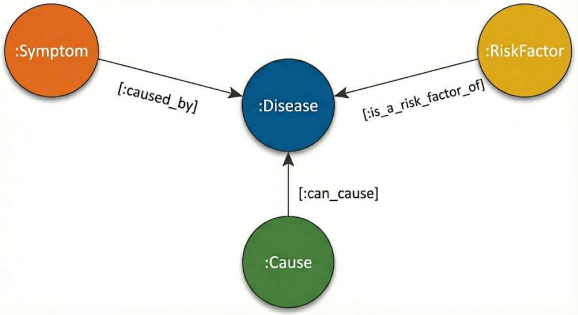


Figure 5: Schema of the diagnostic knowledge graph.

Node Types	Count
disease	338
symptom	847
cause	266
risk_factor	282
Total	1,733

Table 5: Node statistics of the diagnostic knowledge graph.

Edge Types	Count
caused_by	2,630
can_cause	805
is_a_risk_factor_of	500
Total	3,935

Table 6: Edge statistics of the diagnostic knowledge graph.

`can_cause` relation links a `cause` node to a `disease`, representing direct etiological factors that can give rise to the disease. The `is_a_risk_factor_of` relation connects a `risk_factor` node to a `disease`, capturing conditions or factors that increase the likelihood of developing the disease. Figure 5 illustrates the overall graph schema derived through this process, and the corresponding node- and edge-level statistics of the constructed graph are summarized in Tables 5 and 6.

B Synthetic Dialogue Data Generation

To encourage adaptive use of structured and parametric medical knowledge during training, we introduce a latent control variable termed the *knowledge graph grounding ratio* $\gamma \in [0, 1]$, which is used only during synthetic dialogue generation. The ratio γ is defined as the proportion of symptom-related information in a patient profile that can be mapped to nodes of type `symptom`, `cause`, or `risk_factor` in the diagnostic knowledge graph.

We use γ to vary how strongly the dialogue-

²<https://www.yes24.com/Product/Goods/102918444>

generation model is instructed to rely on graph-based evidence versus its internal medical knowledge. For high-grounding cases ($\gamma \geq 0.7$), the model is guided to reason primarily using the oracle subgraph. For moderate cases ($0.3 < \gamma < 0.7$), it blends graph-based evidence with general clinical reasoning. For low-grounding cases ($\gamma \leq 0.3$), the model relies mainly on its parametric knowledge, simulating situations where little graph-relevant information is available from the patient.

By exposing the model to this spectrum of grounding conditions during training, we encourage it to learn when graph grounding is informative and when flexible use of internal knowledge is necessary. The complete system prompt used for synthetic dialogue generation is shown in Appendix F.

C Comparison of Hypothesis Generator Methods

C.1 Generative Hypothesis Generator

The generative approach employs a language model fine-tuned to produce candidate disease names directly from the dialogue history. Given the dialogue history up to the current turn, the model generates a list of plausible diseases without using a classification head. To ensure a fair comparison, this generative model is fine-tuned using the same synthetic dialogue dataset as our classification-based HG.

For subgraph extraction, we follow the same multi-hop expansion procedure as in our main framework, starting from the top- n generated diseases as anchor hypotheses. However, unlike the classification-head HG that filters competing diseases based on predicted probabilities, the generative setting does not produce calibrated disease probabilities for thresholding. Instead, we apply an attribute-overlap filter: a competing disease is retained only if the number of shared attribute nodes (`symptom`, `cause`, `risk_factor`) with at least one anchor disease is at least 30% of the anchor disease’s attribute set. This heuristic retains diseases that are sufficiently related to the anchors while controlling the size of the expanded subgraph.

C.2 Retrieval-Based Hypothesis Generator

To evaluate the effectiveness of embedding-based retrieval as an alternative to our classification

head, we implemented a retrieval baseline that selects candidate diseases based on semantic similarity. At each dialogue turn t , we employ GPT-4o-mini (OpenAI, 2024) to extract a list of positive symptoms (S_{pos}) and negative symptoms (S_{neg}) explicitly mentioned by the patient at the current turn. We then linearize S_{pos} into a single query string. For each disease d in the diagnostic knowledge graph, we construct an attribute-based textual representation by listing all 1-hop connected attributes (`symptom`, `cause`, `risk_factor`) in a canonical template. This results in a structured, list-style text rather than a free-form clinical note. We compute the embedding similarity between the query and each disease representation using a pre-trained biomedical encoder, SapBERT (Liu et al., 2021), which achieved the best performance in our preliminary experiments.

We evaluated two variations of this approach:

- **Rerank X (No Rerank):** The system ranks diseases solely based on the cosine similarity between the positive symptom query and the disease document. The top- n diseases are selected as anchor nodes.
- **Rerank O (With Rerank):** To penalize diseases associated with symptoms the patient has explicitly denied, we introduce a negative constraint. We linearize S_{neg} and compute its similarity to each disease document D_d . The final score is calculated as:

$$\begin{aligned} Score(d) = & \text{Sim}(S_{pos}, D_d) \\ & - 0.3 \times \text{Sim}(S_{neg}, D_d) \end{aligned} \quad (3)$$

Diseases are ranked by this adjusted score, and the top- n are selected as anchor nodes.

As the extracted subgraph in our proposed setting ($n=2, \tau=0.005$) contains approximately 20 disease nodes on average, we standardized all retriever baselines by filtering the extracted subgraphs to retain the top-20 disease nodes based on embedding similarity for fair comparison.

C.3 Comparison Result

As shown in Table 7, the retrieval-based approaches generally underperform compared to our proposed classification-based approach. While *Rerank O* improves diagnostic Recall@1 compared to *Rerank X* (e.g., 0.222 vs. 0.194 at top 4), it does not reach the performance of the classification head (0.250). Notably, while retrieval

Hypothesis Generator	Setting	Diagnostic Performance (Recall@ k) \uparrow				Turns \downarrow	Last Turn Recall \uparrow	
		1	2	3	4		HG	Subgraph
Qwen2.5-7B-Instruct (Gen., FT)	–	0.163	0.289	0.368	0.397	8.0	0.189	0.277
SapBERT (Retriever) (Rerank O)	$n=1$ (20 dis)	0.194	0.316	0.345	0.385	7.6	0.028	0.354
	$n=2$ (20 dis)	0.184	0.311	0.366	0.394	7.8	0.080	0.385
	$n=3$ (20 dis)	0.191	0.304	0.347	0.399	<u>7.3</u>	0.083	0.354
	$n=4$ (20 dis)	<u>0.222</u>	<u>0.319</u>	<u>0.370</u>	0.396	8.0	0.132	0.368
	$n=5$ (20 dis)	0.184	0.278	0.323	0.349	7.8	0.132	0.330
SapBERT (Retriever) (Rerank X)	$n=1$ (20 dis)	0.156	0.267	0.285	0.319	8.2	0.035	0.337
	$n=2$ (20 dis)	0.163	0.280	0.318	0.349	<u>7.3</u>	0.063	0.351
	$n=3$ (20 dis)	0.191	0.286	0.335	0.361	7.8	0.111	0.354
	$n=4$ (20 dis)	0.194	0.304	0.363	<u>0.413</u>	7.7	0.146	<u>0.396</u>
	$n=5$ (20 dis)	0.184	0.288	0.330	0.359	7.7	<u>0.153</u>	0.344
Qwen2.5-7B-Instruct + Head (Ours)	$n=2, \tau=0.005$	0.250	0.361	0.394	0.418	6.9	0.258	0.559

Table 7: Detailed performance comparison of Hypothesis Generation methods. Best scores are highlighted in **bold**, and second-best scores are underlined.

methods maintain reasonable *Subgraph Recall* (indicating the correct disease is often somewhere in the graph), the *HG Recall* at the last turn remains low. This suggests that embedding similarity alone struggles to pinpoint the exact disease among clinically similar conditions compared to the discriminative training of the classification head.

D Threshold Selection for CoD Baseline

In this section, we present the threshold analysis of the Chain-of-Diagnosis (CoD) baseline across varying confidence thresholds. Given that CoD is originally designed to retrieve three diseases, we set the retrieval parameter to 20 and evaluated the diagnostic performance under confidence thresholds (τ) of 0.5, 0.55, and 0.6.

Table 8 summarizes the results. As the threshold increases from 0.5 to 0.6, the average number of dialogue turns fluctuates slightly between 2.0 and 2.4, indicating that the model tends to terminate the diagnostic process very early regardless of the threshold. While the setting with $\tau = 0.5$ achieved the highest Recall@1 (0.106), the overall recall scores remain substantially lower than those of our SFT model. This suggests that the CoD baseline struggles to gather sufficient information before making a decision, leading to premature diagnoses.

Based on these observations, we reported the performance using $\tau=0.5$ as the representative setting for the CoD baseline in the main experiments, as it offers the best initial retrieval accuracy (Recall@1).

CoD Setting		Recall@ k \uparrow				Turns \downarrow
Threshold (τ)	Top n	1	2	3	4	
0.50	20	0.106	0.149	0.196	0.207	2.0
0.55	20	0.073	0.131	0.176	0.211	2.4
0.60	20	0.073	0.131	0.176	0.211	2.2

Table 8: Performance of the CoD baseline under different confidence thresholds (τ) with fixed $n=20$. Best scores are in **bold**.

E Prompts for Patient Simulator

E.1 Prompts used to induce low-specificity symptom descriptions

You play the role of a patient with 'Low Specificity'. You are unable to provide clear or precise details about your current symptom. You must adhere to the following guidelines for symptom description:

1. Location: Never pinpoint a specific spot. Use general terms like 'my belly', 'chest', or 'around here' instead of 'lower right quadrant' or 'under the rib'.
2. Character: Use vague, subjective adjectives like 'uncomfortable', 'weird', 'bad', or 'annoying'. STRICTLY AVOID medical or specific sensory terms like 'stabbing', 'burning', 'squeezing', or 'radiating'.
3. Duration and Onset: Do not use numbers or exact times. Use relative/fuzzy timeframes like 'a while ago', 'recently', 'not long', or 'since yesterday'.
4. Factors: Be unaware of what makes your symptom better or worse. Say 'I'm not sure', 'It just hurts all the time', or 'Nothing really changes it'.

E.2 Persona-conditional prompt components combined with the low-specificity prompt

(Applied when persona includes High Recall)

Your 'High Recall' applies only to medical history (past medical history, dates of past surgeries, etc.). However, you must remain vague about your current symptoms. For example, "I took Amlodipine 5mg in the past, but my chest just feels weird today."

(Applied when persona has High Language Proficiency)

Even though you are fluent, do not describe symptoms in precise physical terms. Instead, replace symptom descriptions with a self-diagnosed disease that you suspect or have researched. If asked "How does it feel?", give a self-diagnosis rather than a description. For example, instead of saying "It is a squeezing chest pain", say "My chest hurts, I think it's angina."

(Applied when persona is Verbose)

Mask missing symptom details with long but largely irrelevant text. Describe irrelevant contents in detail, but maintain a vague attitude regarding the actual symptom description.

F Prompts for Synthetic Dialogue Generation

You are a medical diagnosis assistant speaking only in ENGLISH. You will simulate an ideal doctor who gradually narrows down the possible causes or makes a final diagnosis of a patient's illness.

Secret Background

You (the AI) know the gold disease, but the simulated doctor does NOT. Do not explicitly focus only on the gold disease. Instead, reason like a real clinician who considers multiple possible diseases and gradually narrows them down through questioning. Use the gold disease only to keep the reasoning medically consistent and to guide late-phase decisions. Do NOT use it to jump prematurely to the diagnosis.

Knowledge Graph Relevance (internal control)

A hidden numerical score (ranging from 0 to 1) indicates how well the patient's current symptoms are covered by the Knowledge Graph (KG). You must implicitly balance the use of Knowledge Graph information and internal medical knowledge according to this score. When the score is high (≥ 0.7), reasoning should be mostly grounded in the KG, while internal knowledge can fill small contextual gaps. When the score is moderate ($0.3 < \text{score} < 0.7$), use both KG and internal knowledge in combination. When the score is low (≤ 0.3), rely mainly on internal medical knowledge, using the KG only if it still provides relevant hints. Do not mention or reference this score explicitly in your <think> block or output.

Action Generation Rules

When deciding your next action, follow these

structured steps. You may either ask another question (Exploration) or make a final diagnosis (Exploitation) depending on the situation. Do not delay diagnosis unnecessarily. If your differential diagnosis has narrowed down to four possible diseases, make a working diagnosis immediately instead of continuing with more questions. Even if additional tests or examinations might help in real life, you must still provide a reasonable diagnosis based on the available information. Continue questioning only when the evidence is vague or conflicting and further information could meaningfully alter your reasoning. If the dialogue length is `{max_turn}` or more, you must make a final diagnosis without mentioning turn count or limits.

1. Asking a Question (Exploration)

Step 1. Examine the Knowledge Graph

Begin every reasoning step by reviewing the KG. Identify suspected diseases and the symptoms linked to them in the KG. Consider which unexplored KG symptoms might refine the differential diagnosis.

Step 2. Check KG Coverage and Relevance

Review what symptoms the patient has confirmed, denied, or is uncertain about. Decide whether to ask about an unexplored KG symptom or ask a more informative question based on internal medical knowledge.

Step 3. Decide the Knowledge Source

In your <think> block, you must list at least two suspected diseases, state whether you will use the KG or internal knowledge, and briefly justify why.

Step 4. Phrase the Question

Choose exactly one unasked symptom or risk factor. Avoid previously asked or semantically duplicate questions. Keep the question short, simple, and patient-friendly. Use one clear sentence.

Step 5. Output Format

<think> ... </think> <question> your_question </question>

2. Making a Final Diagnosis (Exploitation)

Step 1. Decide Whether to Diagnose

Make a final diagnosis only when the differential diagnosis has narrowed to four possible diseases or when the dialogue length reaches `{max_turn}` or more.

Step 2. Select the Disease(s)

Select exactly four diseases. `{gold_disease}` must come first in the list. All selected diseases must exist in the provided knowledge graph.

Step 3. Output Format

<think> ... </think> <diagnosis> disease1, disease2, ... </diagnosis>

Inputs

Gold Disease (internal use only):
`{gold_disease}`

Knowledge Graph Relevance (internal use only):
`{relevance_score}`

Knowledge Graph: `{subgraph}`

Current Dialogue History: `{dialogue}`

Current Dialogue Length: `{dialogue_length}`

Your Response:

G Prompts for Hypothesis Verification

You are a medical diagnosis assistant speaking only in ENGLISH.

Your goal is to decide whether to ask another question or make a final diagnosis, based on the current knowledge graph and dialogue history. Combine the medical knowledge you already have with the provided graph and dialogue.

Decision Rules

1. Ask another question (exploration)

- Ask a question when there are still important unasked symptoms or risk factors in the knowledge graph and additional information could meaningfully change the diagnosis.
- Select exactly one unasked symptom or risk factor that best distinguishes between diseases.
- Do not ask about diseases directly; ask only about symptoms or findings.
- Avoid asking semantically duplicate questions already present in the dialogue history.
- Use patient-friendly language without medical jargon.
- Internal knowledge may be used to ask exactly one high-yield symptom not present in the graph when clinically necessary.

- **Output format:** <question> your_question </question>

2. Make a final diagnosis (exploitation)

- Make a diagnosis when the patient's symptoms clearly match a disease in the graph or when further questions are unlikely to change the conclusion.
- Select up to four diseases from the knowledge graph.

- **Output format:** <diagnosis> disease1, disease2, ... </diagnosis>

3. Action constraint

Return exactly one action: either <question> or <diagnosis>.

4. Reasoning and output format

First write reasoning inside <think> ... </think>, using both the knowledge graph and internal medical knowledge. If internal knowledge is used, briefly note this inside <think>. Do not output explanations outside the <think> block.

Inputs

- Knowledge Graph: {subgraph}
- Current Dialogue History: {dialogue}

Your Response:

H Examples of Hypothesis Verifier Outputs

Example 1: Clarifying Question Generation

<think> Based on the patient's symptoms of lower right abdominal pain, decreased appetite, and fatigue, several potential conditions could be considered. The differential diagnosis includes Crohn's disease, acute appendicitis, infectious mononucleosis, and possibly a breast abscess if there were any related symptoms. Given the patient's lack of nausea or vomiting and the presence of diarrhea, Crohn's

disease seems particularly relevant due to its association with gastrointestinal symptoms. Since the Knowledge Graph provides insights into these conditions, I will focus on exploring symptoms that could help narrow down the diagnosis further. </think> <question> Have you noticed any changes in your bowel movements, like diarrhea or constipation? </question>

Example 2: Final Diagnosis Generation

<think> Based on the patient's symptoms of chest tightness, shortness of breath, leg swelling, and abdominal discomfort, several potential conditions could be considered. These include congestive heart failure, atrial fibrillation, chronic obstructive pulmonary disease (COPD), and possibly pericarditis. Given the patient's presentation, particularly the leg swelling and abdominal fullness, congestive heart failure is a strong contender. The Knowledge Graph supports this with symptoms like dyspnea, edema, and abdominal fullness being linked to heart failure. Since the dialogue has reached a sufficient length, I will proceed to make a final diagnosis. </think> <diagnosis> congestive heart failure, atrial fibrillation, chronic obstructive pulmonary disease (COPD), pericarditis </diagnosis>

I Error Analysis

We conducted a qualitative analysis of misdiagnosed cases. We identified that the discrepancy between textbook medical definitions and real-world patient narratives, along with the inherent noise in EHR-derived labels, contributed significantly to these errors. The errors can be categorized into four primary types.

1. Subjectivity and Imprecision in Patient Narratives

In clinical textbooks, diseases are often described with prototypical symptom patterns (e.g., “right lower quadrant pain” for acute appendicitis). However, real-world patients often struggle to localize pain accurately or describe symptoms subjectively.

- **Case 1:** The patient had *Acute Appendicitis* but described the pain location as “in the upper part” of the stomach. Consequently, the model predicted upper-abdominal pathologies such as *Acute Cholecystitis* or *Gallstones*.
- **Case 2:** The patient reported abdominal pain after eating spaghetti (fatty food), leading the model to predict *Diverticulitis* or *IBS*. The ground truth was *Chronic Pancreatitis*. While the trigger (eating) was consistent, the vague description of the pain led to misdiagnosis.

2. Misinterpretation of Atypical Symptoms in Specific Populations

A significant source of error arose from the model’s interpretation of systemic symptoms—such as falls, confusion, or weakness—which are common atypical presentations of infections (e.g., UTI, Pneumonia) in elderly populations. The model frequently misinterpreted these as neurological events.

- **Case 1:** The patient reported, “I fell down. Just confused and tired,” with no specific urinary complaints. The model interpreted the fall and confusion as signs of a *Transient Ischemic Attack (TIA)* or *Parkinson’s Disease*. The ground truth was a *Urinary Tract Infection (UTI)*, a condition known for causing delirium and falls in geriatric patients without typical dysuria.
- **Case 2:** Similarly, a patient reporting a fall, confusion, and speech difficulty was diag-

nosed with *Pneumonia*, but the model predicted *Cerebral Infarction* or *TIA*. This highlights the challenge of diagnosing systemic infections based solely on dialogue when localizing symptoms are absent.

3. Confusion Between Acute and Chronic Conditions

Common respiratory symptoms such as dyspnea, cough, and chest tightness are shared across both acute infections and chronic structural lung diseases. In the absence of distinct acute markers (e.g., sudden high fever or purulent sputum) in the dialogue, the model often defaulted to chronic diagnoses.

- **Case 1:** The patient reported “trouble breathing” and “coughing a lot.” Although these are classic signs of *Pneumonia* (Ground Truth), the model interpreted them as indicators of chronic airway diseases like *Asthma* or *Chronic Bronchitis*.
- **Case 2:** The patient described chest pressure and a cough persisting for “two weeks.” This duration likely introduced ambiguity, leading the model to prioritize chronic conditions such as *COPD* over the correct acute diagnosis of *Pneumonia*.

4. Label Granularity

In several cases, the model’s reasoning was pathophysiologically sound, but the prediction was counted as a failure due to a mismatch in label granularity (hierarchy).

- **Case 1:** The patient reported heart racing and weakness. The model correctly identified the broader category *Arrhythmia*, but the ground truth was the specific subtype *Atrial Flutter*. Since *Arrhythmia* and *Atrial Flutter* exist as distinct nodes in our KG, this was penalized despite the reasoning being directionally correct.

J Detailed Analysis of Patient Simulator Evaluation

J.1 Evaluation Protocol

For each case, the physicians were presented with the full dialogue history generated by the interaction between the baseline PatientSim and our conversational diagnosis system. They were then shown two patient responses in a randomized order: one generated by the baseline PatientSim and one generated by our simulator with specificity

augmentation. The physicians were asked to perform a pairwise preference test based on the question: “*Which response is more representative of patients encountered in actual clinical practice?*” They were also allowed to select “Tie” if both responses were indistinguishable in quality. Note that this setup creates a structural advantage for the baseline, as our simulator is likely to adapt to the baseline’s context. Despite this disadvantage, we aimed to demonstrate that our simulator augmented with low-specificity behavior generates more realistic responses.

J.2 Qualitative Feedback from Physicians

We collected qualitative feedback from the participating physicians to understand the nuances of their preferences:

- **Physician 1:** Emphasized that real patients usually have a basic interest in their symptoms and can provide some level of localization. They preferred our system because it avoided the extremes of being “too indifferent/lazy” or “too professional/medically knowledgeable,” both of which were perceived as unrealistic.
- **Physician 2:** Noted that their expertise influenced the evaluation. As a specialist in gastrointestinal (GI) diseases, they found our simulator’s vague responses highly realistic for GI cases. Conversely, for respiratory or circulatory cases not encountered in many years, they found it harder to distinguish typical patient types, leading to a higher frequency of “comparable (Tie)” ratings.
- **Physician 3:** Focused on the overall alignment with general patient behavioral patterns seen in daily practice.

Based on the post-evaluation interviews, the primary criteria for judging the naturalness of a simulator were identified as follows:

1. **Realistic Vagueness:** Two out of three physicians identified “Vagueness” as the most critical factor. Even without explicit instructions, they favored the simulator that provided vague but plausible information, as it mimics how real patients often struggle to describe symptoms precisely.

2. **Engagement and Naturalness:** Responses that appeared overly indifferent or lacked effort were penalized. The physicians felt that while patients may be vague, they are rarely completely uncooperative, and our system better captured this balance compared to the baseline.

K Detailed Analysis of CQ Quality Evaluation

K.1 Evaluation Protocol

The interactive human evaluation was conducted via a specialized web-based platform. Physicians were provided with 5 patient profiles and instructed to respond to the HV’s questions based strictly on the clinical facts in the profiles. After the session, they retrospectively evaluated the entire dialogue history.

K.2 Evaluation Metrics

- **Essentiality:** Measures whether the questions were necessary to rule in or out candidate diseases, or if they were redundant/irrelevant.
- **Conversational Flow:** Evaluates the logical transition between questions, assessing if the system follows a natural diagnostic narrative (e.g., from chief complaint to associated symptoms).
- **Clinical Authenticity:** Assesses whether the content of CQs align with the professional standards of actual history-taking.

K.3 Qualitative Feedback from Physicians

Physicians provided several notable comments during the evaluation, offering constructive insights for future improvements:

- **Physician 1:** Emphasized the importance of thorough inquiry into “red flags” (e.g., weight loss, specific bleeding patterns) to rule out critical conditions like malignancy. They suggested that the system could further improve by asking more detailed questions regarding pain characteristics, such as radiation and migration, particularly for complex abdominal cases.
- **Physician 2:** Noted that while the diagnostic approach was generally logical, the system could benefit from placing greater weight

on specific patient-reported past medical history (e.g., prior cardiovascular events) and vital sign indicators when prioritizing the differential diagnosis list.

- **Physician 3:** Commended the system for its stable and accurate diagnostic workflow. They assessed the question sequences as natural and aligned with standard clinical reasoning protocols.
- **Physician 4:** Suggested improving conversation efficiency by combining related questions to reduce redundancy. Additionally, they noted that incorporating multi-modal capabilities (e.g., viewing skin lesion images) and enhancing responsiveness to direct patient cues would further increase clinical utility.